Volume 2, Number 2, pp. 240-247, 2000.

◆ Home Current Issue Table of Contents ▶

# Study of Respiratory Motion of the Heart in Coronary MR Angiography

D. Manke\*, K. Nehrke\*\*, P. Rösch\*\*, and O. Dössel\*

\* Institute of Biomedical Engineering, Universität Karlsruhe, Kaiserstrasse 12, D-76128 Karlsruhe, Germany \*\* Philips Research Laboratories, Devision Technical Systems, Röntgenstraße 24-26, D-22335 Hamburg, Germany

Correspondence: dirk.manke@philips.com

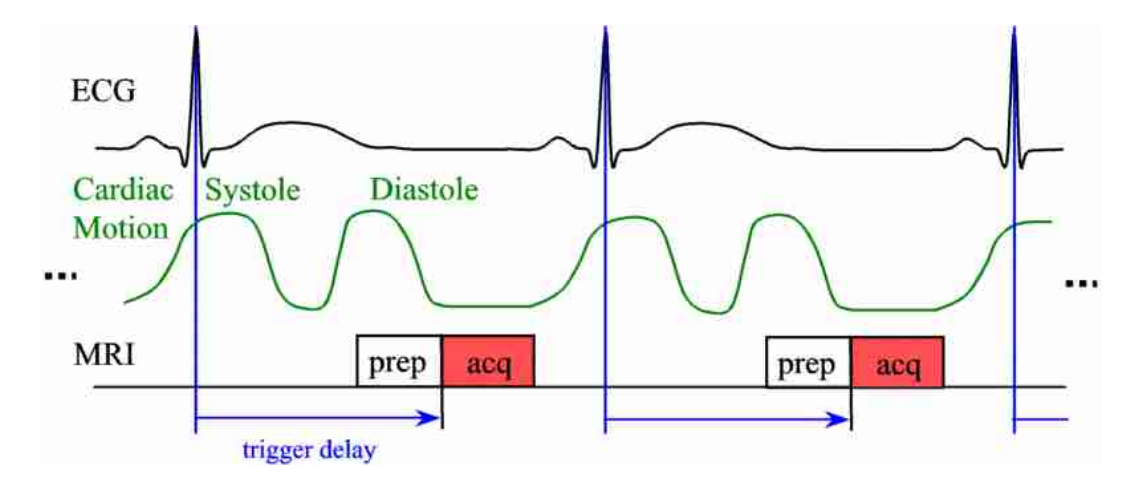
**Abstract.** Motion is one major problem of magnetic resonance imaging (MRI) of the coronary vessels. Despite of cardiac motion of the beating heart itself respiratory motion has to be considered (see MR movie of respiratory gmotion of the heart). Respiratory motion is commonly suppressed by ating techniques, which reduce scan efficiency. In principle modern MR scanners are able to correct those motion patterns prospectively, which can be described by a 3D affine transformation. A prospective motion correction approach could be used to increase the respiratory gating window and in consequence to reduce scan time. However, in order to achieve a sufficient correction the motion must be described quantitatively.

In this initial study the respiratory motion of the heart (coronary vessels) was analysed and a new motion model described by an affine transformation was compared to two rigid motion models. The affine transformation model achieved a better fit (mean error < 1 mm for coronary vessels) than a rigid motion model describing translation in all directions (mean error < 2 mm) and a rigid motion model covering only superior-inferior motion (mean error < 6 mm).

Keywords: MR Angiography, Respiratory Motion, Coronary Arteries

## Introduction

Cardiac and respiratory motion during the data acquisition causes serious ghosting and blurring artifacts in coronary MR imaging. In order to address the motion problem cardiac triggering and respiratory gating have been introduced in standard coronary MR protocols [1,2].



MRI - MR imaging sequence

prep - contrast preparation

acq - data acquisition window (~100 ms)

Figure 1. Cardiac-triggering in a coronary MR scan: data is acquired during middiastole (low cardiac motion) in several subsequent cardiac cycles.

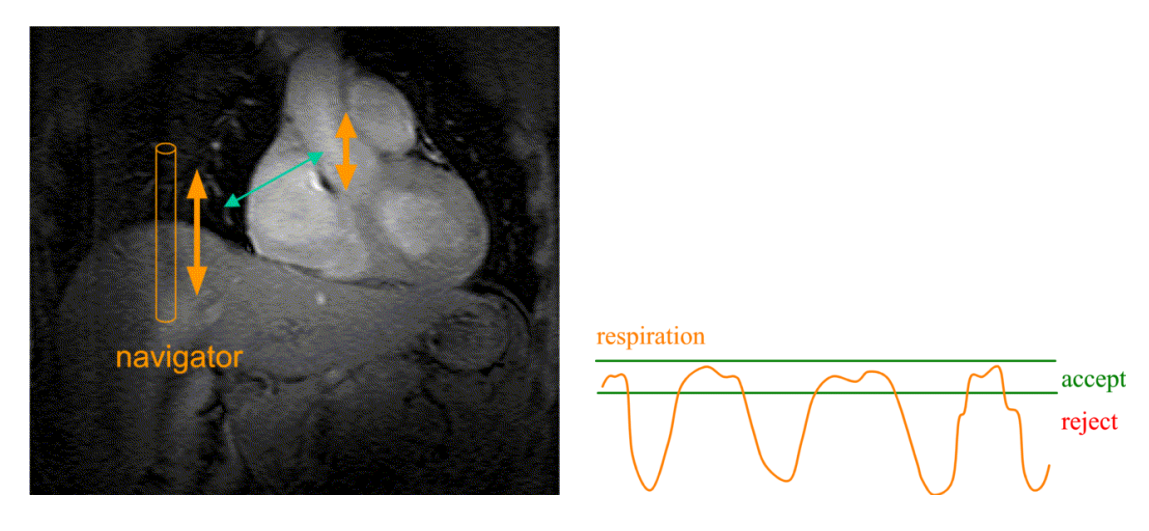


Figure 2. Respiratory gating: Respiratory motion of the right hemidiaphragm is measured during the examination. A linear correlation between motion of the diaphragm and the heart is assumed. Acquired data is only accepted if the navigator position is in the respiratory gating window. Otherwise data is rejected and has to be remeasured.

Since only a short time window of ~100 ms is used for data acquisition in the cardiac R-R interval (~1000 ms) cardiac imaging suffers from low scan efficiency and long scan times. Scan time is further increased by a factor of 2 to 3 by the use of respiratory gating. In consequence a high resolution 3D scan of one coronary vessel for example lasts approximately 10 to 15 minutes.

Prospective motion correction, which is done in real-time during data acquisition, provides the opportunity to increase the respiratory gating window without loss of image quality. Up to now, only translation of the heart in superior-inferior direction is corrected in common cardiac MR examinations by using a rigid-body-motion model (slice-tracking). However, prospective motion correction in MRI provides the capability to perform corrections based on the more general affine transformation model. In the present work the feasibility of this model for respiratory motion of the heart was studied.

## **Methods**

## **Imaging**

Experiments on several healthy volunteers were performed on a clinical scanner (Philips ACS-NT15). The proximal portions of the right coronary artery (RCA) and the left anterior descending artery (LAD) were imaged in different respiratory phases. A standard segmented k-space 3D gradient echo sequence was used (TR = 8.6 ms, TE = 3.2 ms, flip angle =  $30^{\circ}$ ). 20 slices were acquired per 3D stack (FOV =  $360x270 \text{ mm}^2$ , slice thickness = 1.5 mm, 512x384 matrix).

A T2-preparation pulse and a fat-saturation pulse were applied for contrast enhancement.

Respiratory motion was monitored by a pencil beam navigator placed through the right hemidiaphragm. In order to cover different respiratory phases the navigator gating window was shifted from end-expiration towards inspiration for subsequent scans. Two corresponding images of the RCA of one volunteer are shown below.

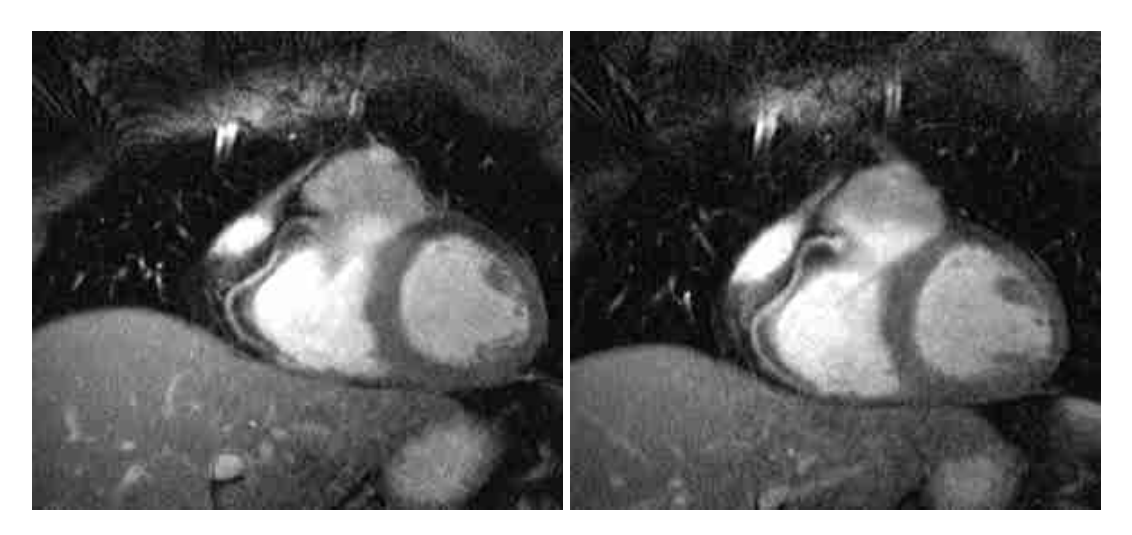


Figure 3. The RCA of one healthy volunteer for end-expiration (left) and inspiration (20mm shift of the right hemidiaphragm) (right).

## **Motion Registration**

For motion registration the images acquired in end-expiration were chosen as reference. In these reference images several characteristic landmarks were selected manually. Corresponding landmark positions for the inspiratory motion states were registered automatically using a block matching algorithm [3].

#### **Motion Models**

Two sets of corresponding landmark positions for end-expiration and inspiration were used to determine the parameters of different motion models for the respiratory motion of the heart. The matrices

$$\begin{split} \mathbf{R}_{ex} &= \{\mathbf{L}_{1,ex}, \mathbf{L}_{2,ex} \dots \mathbf{L}_{n,ex}\} \\ \mathbf{R}_{in} &= \{\mathbf{L}_{1,in}, \mathbf{L}_{2,in} \dots \mathbf{L}_{n,in}\} \end{split} \tag{1}$$

contain corresponding landmark positions for end-expiration (ex) and inspiration (in)

$$\mathbf{L}_{\mathbf{k,ex}} = (x_{k,ex}, y_{k,ex}, z_{k,ex}, 1)^{\mathbf{T}}$$
 and (2)

$$\mathbf{L_{k,in}} = (x_{k,in}, y_{k,in}, z_{k,in}, 1)^{\mathrm{T}}$$

in homogeneous coordinates [4].

The following motion models have been examined:

- (a) Translation only in superior-inferior direction
- (b) 3D translation
- (c) 3D affine transformation (translation + linear transformation)

Parameters for the translational motion models (a) and (b) were calculated by taking the mean values of the x,y,z-components of the difference vectors between corresponding landmarks:

$$\overline{\Delta \mathbf{L}} = \sum_{k=1}^{n} \left( \mathbf{L}_{\mathbf{k,in}} - \mathbf{L}_{\mathbf{k,ex}} \right) / n \tag{3}$$

The optimum parameters for the affine transformation model (c) described by square matrix **Acorr** were determined by

$$\mathbf{A_{corr}} \cdot \mathbf{R_{in}} \stackrel{!}{=} \mathbf{R_{ex}} \quad \Rightarrow \quad \mathbf{A_{corr}} = \mathbf{R_{ex}} \cdot \mathbf{R_{in}}^{\mathsf{T}} (\mathbf{R_{in}} \cdot \mathbf{R_{in}}^{\mathsf{T}})^{-1} \quad (4)$$

The affine transformation **Acorr** maps the inspiratory motion state (in) to the end-expiratory reference state (ex).

## **Results**

During tidal breathing (up to 20 mm diaphragm shift) the RCA is shifted up to 10 mm in superior-inferior direction, which is the 3fold diameter of the coronary vessel. While anterior-posterior motion seems to be irrelevant for the RCA for tidal breathing (shift < 1 mm for this volunteer) , the RCA moves  $\sim 5$  mm to the right during inspiration of this volunteer. Displacements for LAD are similar (9.1 mm inferior, 3.0 mm anterior, 4.0 mm right) except anterior motion, which is approximately the diameter of the vessel.

Linear deformations can be observed especially for the RCA, where linear expansion in superior-inferior direction seems to be the most important component.

For LAD these linear deformations are not as strong as for RCA but are still relevant.

#### Comparison of Motion Models

Landmarks found for RCA and LAD of one volunteer for end-expiration and inspiration (20 mm shift of the right hemidiaphragm) were used for the 3D plots shown below (Figure 4, Figure 5, Figure 6).

#### (a) Translation in superior-inferior direction:

This motion model is commonly used in coronary MR examinations, where a fixed correction factor between right hemidiaphragm and heart is used [5]. In this example a mean displacement in superior direction of each vessel was calculated with equation (3) (RCA: 10.3 mm, LAD: 9.1 mm) and applied for correction. The corrected vessels do not fit very well to the reference state, the mean distance between corresponding landmarks is still 5.9 mm for RCA and 5.1 mm for LAD.

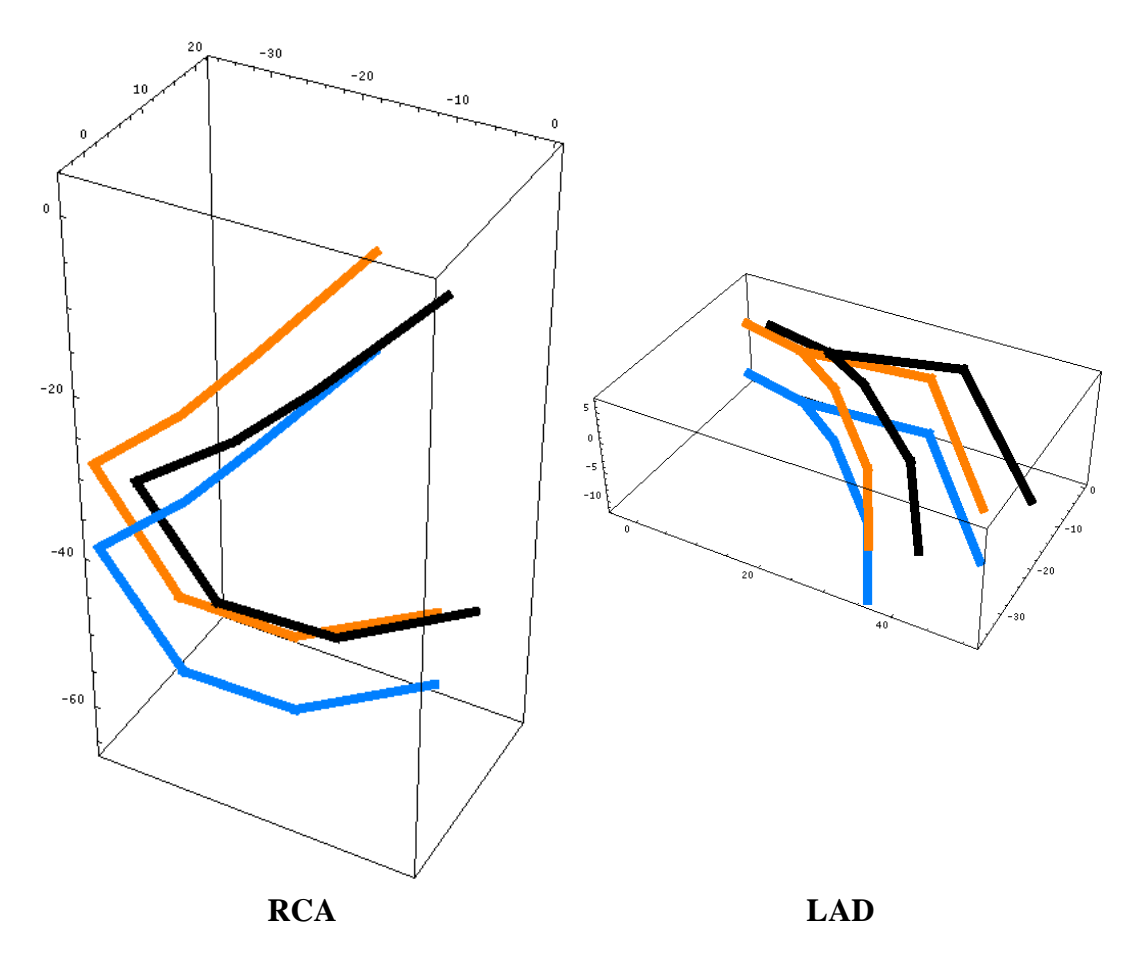


Figure 4. Coronary vessels in different respiratory states (end-expiration (black), 20mm inspiration (blue)) and correction of superior-inferior translation (orange).

## (b) 3D Translation:

A better fit can be achieved by a model that considers all components of translation. The mean displacement for each vessel (RCA: 10.3 mm inferior, 0.1 mm anterior, 5.5 mm right; LAD: 9.1 mm inferior, 3.0 mm anterior, 4.0 mm right) was calculated using equation (3) and applied for correction. The mean distances between corresponding landmarks of the corrected vessels and the reference state are 1.9 mm for RCA and 1.3 mm for LAD.

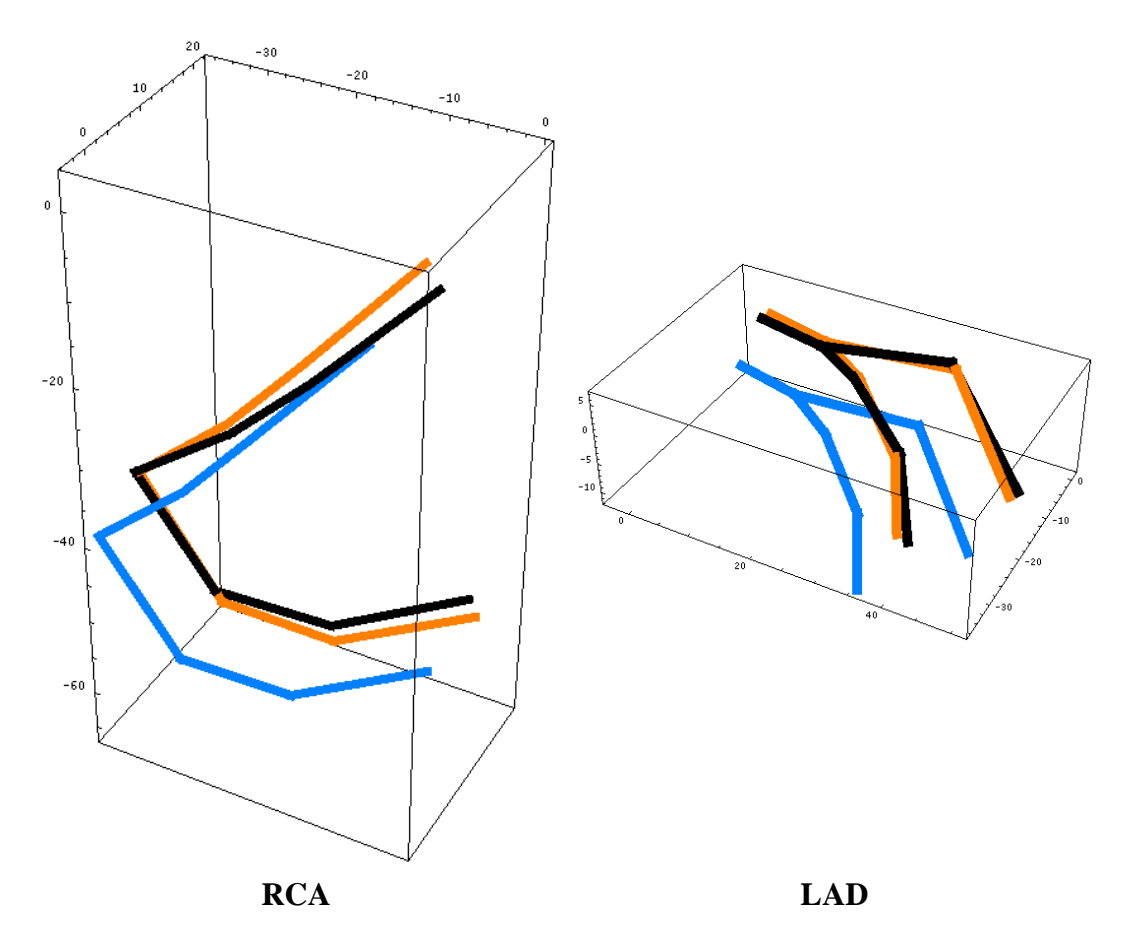


Figure 5. Coronary vessels in different respiratory states (end-expiration (black), 20mm inspiration (blue)) and correction of 3D translation (orange).

## (c) 3D affine transformation:

Best results were achieved using a 3D affine transformation model since it provides most degrees of freedom. Model parameters were determined using Equation (4). The mean distances between corresponding landmarks of the corrected vessels and the reference state are 0.3 mm for RCA and 0.4 mm for LAD in this example, which is significantly below the vessel diameter.

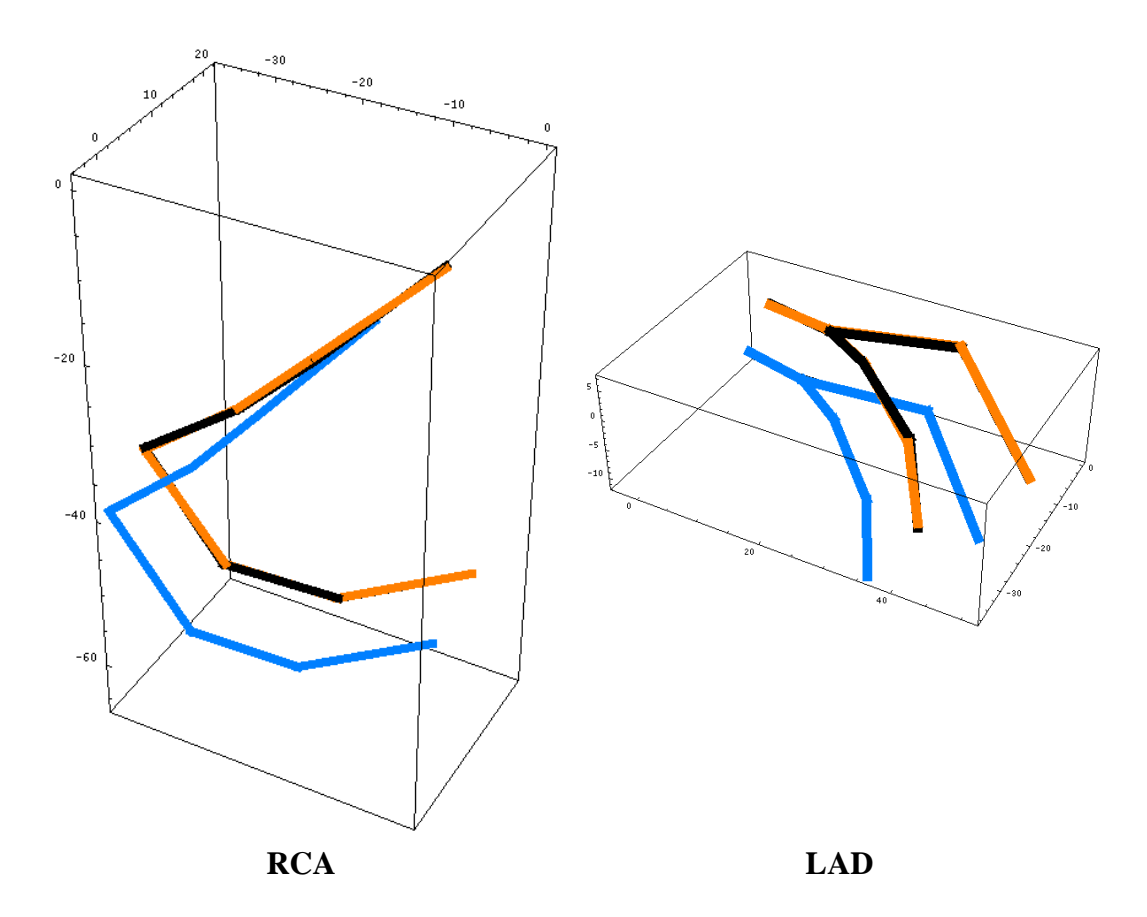


Figure 6. Coronary vessels in different respiratory states (end-expiration (black), 20mm inspiration (blue)) and correction of affine transformation (orange).

## **Conclusions**

In the present study respiratory motion of the coronary arteries was examined. The common rigid motion model including only translation in superior-inferior direction is not able to describe respiratory motion of the heart properly. An extension to a 3D translation or a 3D affine transformation improves the model fit significantly.

The motion model could be used for prospective motion correction during high resolution coronary MR scans. In consequence, the respiratory gating window could be increased substantially. This could reduce scan time significantly.

In a clinical application model parameters will have to be determined in a preparation phase in a simpler way than performed in this study. In addition a priori information described by a motion model will have to be used and only a few patient dependent parameters of the model will be adapted.

## References

- [1] Stuber, M. et al., "Double-oblique free-breathing high resolution magnetic resonance angiography", Journal of American College of Cardiology, vol.34, p.524, 1999.
- [2] Sachs, T.S. et al., "Real-time motion detection in spiral MRI using navigators", Magnetic Resonance in Medicine, vol.32, p.639, 1994.
- [3] Rösch, P., Weese, J., Netsch, T., Quist, M., Penney, G.P. and Hill, D.L.G., "Robust 3D deformation field estimation by template propagation", submitted to MICCAI 2000.

- [4] Jähne, B., "Digital image processing", 4th Edition, Springer, 1997.
- [5] Wang, Yi, Riederer, S.J. and Ehman, R.L., "Respiratory motion of the heart: kinematics and the implications for the spatial resolution in coronary imaging", Magnetic Resonance in Medicine, vol.33, p.713, 1995.



Official journal of the International Society for Bioelectromagnetism